Kalman Particle Filter for Lane Recognition on Rural Roads

Heidi Loose, Uwe Franke
Daimler AG
Group Research & Advanced Engineering
heidi.loose, uwe.franke@daimler.com

Christoph Stiller
Institute for Measurement and Control Theory
University of Karlsruhe, Germany
stiller@mrt.uka.de

***Abstract*—Despite the availability of lane departure and lane keeping systems for highway assistance, unmarked and winding rural roads still pose challenges to lane recognition systems. To detect an upcoming curve as soon as possible, the viewing range of image-based lane recognition systems has to be extended. This is done by evaluating 3D information obtained from stereo vision or imaging radar in this paper. Both sensors deliver evidence grids as the basis for road course estimation. Besides known Kalman Filter approaches, Particle Filters have recently gained interest since they offer the possibility to employ cues of a road, which can not be described as measurements needed for a Kalman Filter approach. We propose to combine both principles and their benefits in a Kalman Particle Filter. The comparison between the results gained from this recently published filter scheme and the classical approaches using real world data proves the advantages of the Kalman Particle Filter.**

I. Introduction

Today, lane recognition has a 20 year old history. Most systems on the market are based on Kalman Filters as proposed by Dickmanns et al. in 1986 [1]. Lane markings are detected and used as measurements for an appropriate Kalman Filter. Designed for highway use, this approach has problems on winding rural roads. Since the used clothoid road model does not correspond to the actual lane, the Kalman Filter may lose track due to wrong predictions. Bad road conditions and poor lane markings on rural roads make feature detection difficult. In 2001, Southall and Taylor [2] presented an approach using a robust estimation scheme, a variant of the Particle Filter, for lane recognition in difficult scenarios. Even if Southall used only markings, the filter provides the possibility to utilize additional cues for lane recognition. In [3] Apostoloff and Zelinsky described an algorithm which fuses lane markings, edges, and the color of the road. Besides different cues from an image sensor, Smuda et al. [4] used a digital map to estimate the road course up to 100 m ahead. In [5] we presented an algorithm which estimates the lane without any markings. Danescu et al. used a Particle Filter for lane tracking in difficult scenarios [6]. Their algorithm utilizes edges, markings, and curbs to weight the particles. Pitch angle detection was separated to reduce the number of necessary samples. Meis and Schneider [7] estimated a road course based on data from an imaging radar sensor. Serfling et al. [8] computed a road shape from a digital map to match it with the visible road in the camera image. Data from an imaging radar sensor and a camera were combined to perform this matching.

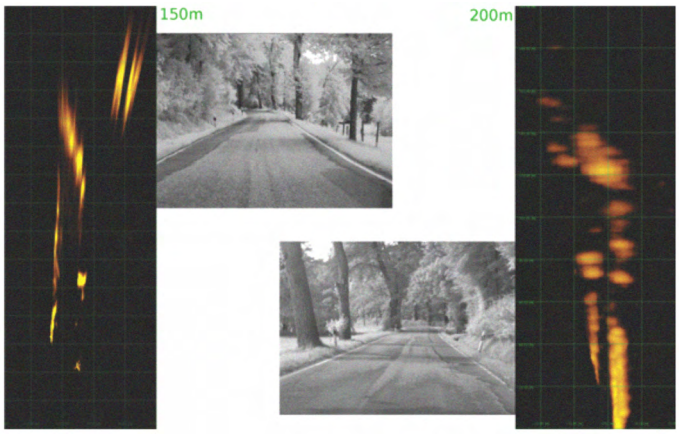

Fig. 1: Evidence grids: The road course is detected with measurements of the three dimensional scene. The left evidence grid shows the stereo measurements of the scenario in the upper camera image, the right grid shows the radar measurements of the scenario in the lower image.

Analyses revealed that the Particle Filter is sensitive in terms of the variances used for spreading the particles in the parameter space. If the variances are too large, the Particle Filter loses its filter effect and the dynamic dependencies are not taken into account. If the variances are too small, the search space is limited and a better solution outside this space is not found. We propose a combination of Kalman and Particle Filter to eliminate the problems of the local limitation of the Kalman Filter and of the choice of variances in the Particle Filter.

The approach presented in this paper has been developed in the context of non-marked rural roads. Compared to our previous approach [5] the viewing range is extended up to 120 m by using 3D information from evidence grids. These grids, as shown in Figure 1, are obtained from an imaging radar sensor or a dense stereo vision system.

In Section II the underlying road model is introduced. Section III sketches the Kalman and the Particle Filter and introduces the Kalman Particle Filter approach. In Section IV the radar and stereo evidence grids are explained. Section V describes the way of finding the measurements used in the Kalman Filter correction step and the cues for weighting the particles. In Section VI we compare the new filter to the two

978-1-4244-3504-3/09/$25.00 ©2009 IEEE

classical approaches on a rural road with a non-clothoidal narrow curve.

II. Road Model

The approach described in the following sections uses the well known clothoid model, introduced in [1].

$$x(L) = \pm 0.5b - x_{\text{offset}} + \Delta\psi L + \frac{1}{2}c_0 L^2 + \frac{1}{6}c_1 L^3 \qquad (1)$$

At the distance L the lateral positions of the lane boundaries are described by Equation (1). The road and the position of the car relative to the road are given by the lane width b, the lateral position of the car to the middle of the road x_{offset}, the yaw angle of the car to the road $\Delta\psi$, the curvature c_0 and the clothoid parameter c_1, which corresponds to the variation of the curvature. These parameters form the state vector $\vec{s}$. For the projection of the lane into the camera image, the height and the pitch angle of the camera have to be measured or observed. The state vector is predicted using the velocity v and the yaw rate $\dot{\psi}_{\text{veh}}$ from the inertial sensors of the car.

III. Filter Algorithms

Two types of filters commonly form the basis of lane recognition approaches: The Kalman Filter, which is the basis for current lane departure warning and lane keeping systems, and the Particle Filter, which was proposed for lane recognition in difficult scenarios.

For the usage in a lane recognition system for winding rural roads both filters are combined in the Kalman Particle Filter. The intention is to exploit the advantages of the Kalman and the Particle Filter, which are shortly described in this section.

A. Kalman Filter

The Kalman Filter estimates a state vector of a dynamic system together with its error covariance matrix. After an initialization this is performed in two steps, see Figure 2. First the state vector $\vec{s}$ and the error covariance matrix P are predicted into the current point in time. Secondly, the predicted state vector is corrected using appropriate measurements and the error covariance matrix is recomputed. A detailed description is given in [9].

The Kalman Filter assumes that the correct state is close to the predicted state, therefore only a local search for measurements is necessary. The Filter applied for lane recognition and tracking using the clothoid road model expects continuously changing road courses. However, the state parameter c_1, which corresponds to the curvature variation, changes abruptly. On highways this variation is small and the error from the road model is negligible. On rural roads the variation of c_1 is significant, which can lead to problems in the lane tracking algorithm. The Kalman Filter tracking fails due to wrong predictions.

Furthermore, the filter has the disadvantage that it cannot cope with multiple measurements like parallel edges. Every measurement is seen as the unique measurement with an error.

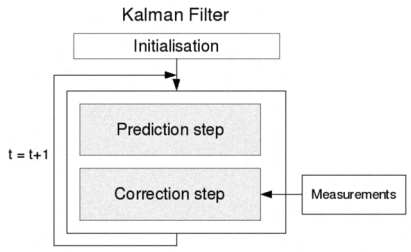

Fig. 2: Kalman Filter: After an initialization the Kalman Filter consists of two steps. Prediction step: The state vector and the error covariance matrix are predicted in the current time. Correction step: The vector and the matrix are corrected using measurements.

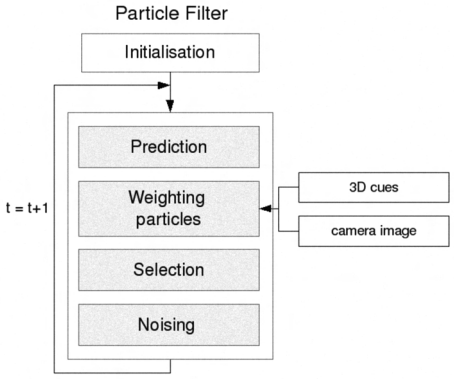

Fig. 3: Particle Filter: In the Particle Filter the predicted particles are weighted using features of the monocular camera image and the evidence grid. In the selection step the particles are suppressed or multiplied depending on the weight and finally a Gaussian noise is added.

B. Particle Filter

A widely used variant of the Particle Filter is the Condensation Algorithm presented by Isard and Blake [10]. It consists of the initialization , where a number of particles are spread over the parameter space, and four steps, which are carried out at each time instant. The algorithm is outlined in Figure 3. At the beginning of one time step, in the prediction step, each particle is predicted into the current time instant. In the weighting step the particles are weighted using a feature F with the calculated likelihood $p(F(x,y)|\vec{s})$ up to a normalization factor. During the selection step the particles are multiplied or suppressed depending on the weight and finally a Gaussian noise is added to each particle. A final estimate is usually formed by the barycenter of the particles.

The variances for the Gaussian noise are set by hand but the behavior of the filter highly depends on these variances. This dependency is the main drawback of the Particle Filter in the application of lane recognition. If the variances are too large, there is no filter behavior and the state vector can change abruptly even if the tracked lane is a good estimation of the actual road course. If the variances are too small, the particles cluster in a small region in the parameter space. In this situation the filter may lose track if the predictions of the particles are wrong.

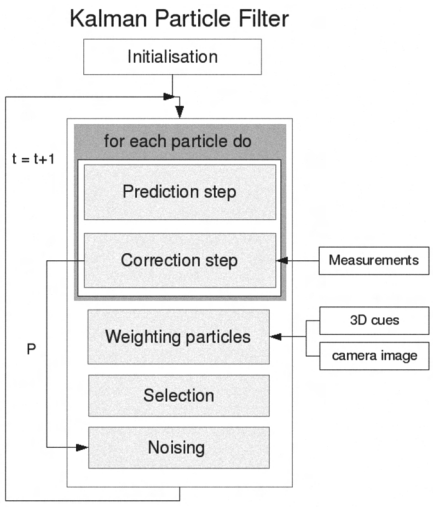

Fig. 4: Kalman Particle Filter: The Kalman Particle Filter performs a Kalman Filter step for each particle. The corrected state vectors are weighted with different cues from the three-dimensional scene and the camera image. In the noising step a Gaussian noise is added to each particle using the variances of the specific error covariance matrix calculated in the Kalman Filter step.

C. Kalman Particle Filter

The Particle Filter manages multiple hypotheses and can also take into account weak cues of the road like color and texture. In contrast to the Particle Filter, the Kalman Filter offers the implicit calculation of the error covariance matrix of the estimated state vector and the correction of the predicted state by measurements.

The Kalman Particle Filter explained by van der Merwe in [11] combines these two filter types to support one another. As seen in Figure 4, the prediction step of the Particle Filter is substituted by a complete Kalman Filter step where each particle is predicted and corrected and its error covariance matrix is calculated. The entries of this matrix are used as variances for the Gaussian noise in the noising step of the Particle Filter. The corrected state vectors are weighted by different cues and selected depending on their weight. The final estimation is deduced from the barycenter of the particles.

Each particle implies a state vector, which defines a lane hypothesis, and its error covariance matrix. Therefore the Kalman Particle Filter can be seen as a multi-hypotheses Kalman Filter approach where the hypotheses are hold by a Particle Filter. Since the state vectors are corrected in the Kalman Filter step and the variances are automatically adjusted, the number of particles can be reduced.

The different sources of information F_i are conditionally independent which leads to the joint probability

$$p(F_1 ... F_n|\vec{s}) = \prod_{i=1...n} p_i(F_i|\vec{s}). \quad (2)$$

IV. Evidence Grids

Image based lane recognition is restricted to a viewing range up to about 60 m. Due to the perspective reduction the resolution in larger distance is not adequate for a robust lane recognition. Therefore we use 3D information represented by evidence grids to extend the viewing range of our lane recognition system. These grids are calculated from imaging radar data or stereo disparities.

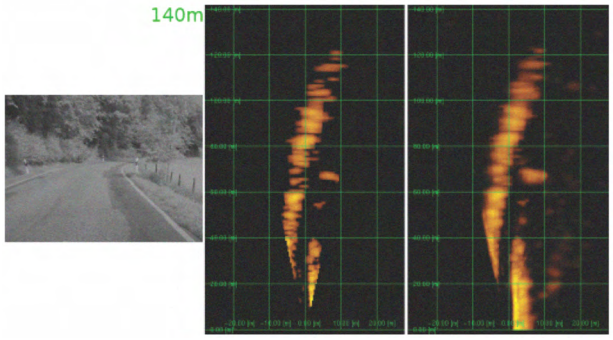

Fig. 5: Radar Evidence Grid: The imaging radar sensor provides the evidence grid (middle) of the scene shown in the camera image. To keep the measurements of the past, the grids were accumulated over time (right).

A. Radar Evidence Grid

The imaging radar provides an intensity image $i(r, \psi)$ and a Doppler image $d(r, \psi)$, with r being the distance and ψ the azimuthal angle. The Doppler value is used to calculate the relative velocity of the reflecting object. In a preprocessing step the moving objects are eliminated in the intensity image to achieve an evidence grid with stationary objects only. Since the road does not reflect the radar beam back in the direction of the transmitter, no measurements will be gained from planar roads. To improve the evidence grid the information is accumulated over time. Obviously, the egomotion has to be compensated. For further processing, the polar evidence grid is transformed in the Cartesian coordinate system, see Figure 5.

B. Stereo Evidence Grid

Modern stereo algorithms deliver dense and precise disparity images, see Figure 6. To calculate the disparities, we use the semi-global matching algorithm presented by Hirschmüller in [15] and improved for long range stereo by Gehrig in [16]. Using this information, an evidence grid is calculated which takes the uncertainties of the stereo measurements into account. The disparity images of two road scenarios and the calculated evidence grids are displayed in Figure 6. Details can be found in [12].

V. Measurements and Weights

In the Kalman Particle Filter approach, cues to achieve for each sample an a posteriori probability to represent the correct road course as well as Kalman Filter measurements are necessary.

The camera image and the evidence grid are used to achieve conditional probabilities. The joint probability for each particle provides the weight needed for the Particle Filter selection step.

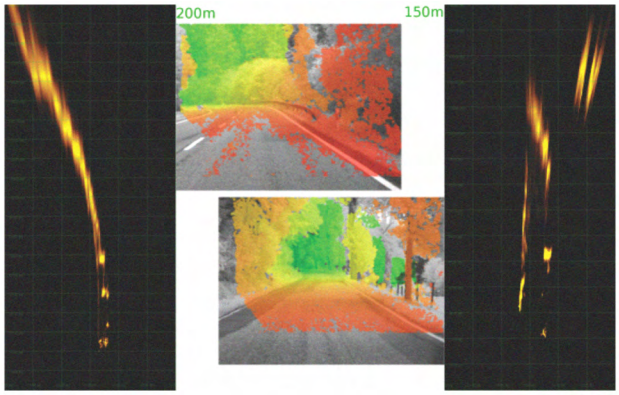

Fig. 6: Stereo Evidence Grid: The left and right images show the stereo evidence grids of different road scenarios. Between the grids the associated disparity images as computed by semi-global matching are shown. The color of the disparity images encodes distance. Red is close and green is far away.

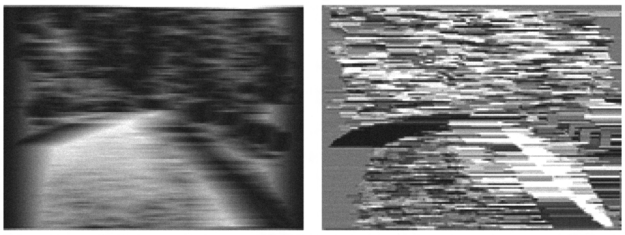

Fig. 7: GDT distance and phase image: For each pixel the distance image (left) encodes the distance to the "most attractive" edge. The darker a pixel, the higher is the probability of being part of the correct lane boundary. The phase image holds the corresponding directions.

A. Camera Image based weighting

Our investigations on Particle Filter based recognition of country roads [5] confirmed that the gradients of the camera image with magnitude and direction are the dominating cues for optical lane recognition even on rural roads. To use the gradients of a camera image for weighting the lane hypotheses, the Generalized Distance Transform (GDT) described in [5] is applied. This algorithm results in two images, a distance image and a direction image, shown in Figure 7. Casually said, for each pixel the distance image encodes the distance to the "most attractive" edge depending on the gradient magnitude, while the phase image stores the corresponding directions.

Based on this distance image D, the conditional probability $p(D|\vec{s})$ is computed by Equation 3.

$$p(D|\vec{s}) = \frac{1}{z_D} e^{-\frac{1}{N} \sum\limits_{(x,y)\in \text{boundaries}} D(x,y)} \tag{3}$$

The number of points along the boundaries is given by N and z_D is the normalizing constant.

The probability of a given road hypothesis is the higher the better the orientation of the lane boundaries matches the data in the phase image. E. g. vertical edges given by trees or reflector posts must not support the lane hypothesis.

The angular difference $\Delta\phi$ between the expected and the assigned angle at each point along the predicted lane boundaries is used to calculate the conditional probability $p(\Delta\phi|\vec{s})$ by Equation 4, with z_ϕ is the normalizing constant.

$$p(\Delta\phi|\vec{s}) = \frac{1}{z_\phi} e^{-\frac{1}{N} \sum\limits_{(x,y)\in \text{boundaries}} -\cos^{2n}(\Delta\phi(x,y))} \tag{4}$$

Good results have been obtained for $n = 5$, while $n = 1$ leads to a weak rating. Considering that the boundaries of the lane seen in the camera image are not the same as the one visible in the evidence grid, the state vector has to be extended by a second lane width and a second lateral position.

B. Evidence grid based weighting

To enlarge the viewing range, features from the evidence grid G are used to calculate a conditional probability for a particle being the correct road $p(G|\vec{s})$. Examining the evidence grids in Figure 1, 5 and 6, the road can be discovered as a region with no measurements, surrounded by two stripes of reflections. To obtain the conditional probability $p(G|\vec{s_i})$, the value of the points inside the road boundaries are integrated and normalized as well as the value of the points of the surroundings, see Equation (5).

$$p(G|\vec{s}) = \frac{1}{z_G} e^{-\left(\frac{1}{N_l} \sum\limits_{(x,y)\in \text{road}} G(x,y) - \frac{1}{N_s} \sum\limits_{(x,y)\in \text{surroundings}} G(x,y)\right)}, \tag{5}$$

where z_G is the normalizing constant. The number of pixels in the lane is characterized with N_l and the number of pixels in the surrounding by N_s.

C. Measurements for Kalman Filter

Since we assume that markings on rural roads are missing, a detection of lane defining features, used as Kalman Filter measurements, is implemented using the 3D information. The road is delimited by stationary objects, which can be found in the stereo as well as the radar evidence grid. The occupied regions form stripes at both sides of the road as seen in Figures 1, 5 and 6. The internal edges of the stripes are used as measurements in the Kalman Filter update step.

VI. Results

A typical poorly marked rural road with a non-clothoidal narrow curve is considered to compare the different filter types utilized for lane recognition. In this sequence, radar evidence grids are used to support the filters, but this could be done using stereo evidence grids as well. Situations of the sequence are exhibited in Figures 8 and 9 to illustrate the behavior of the Particle Filter and the Kalman Particle Filter. The detected road courses are displayed in the radar map and projected into the camera image. The white lines describe the lane using the width and the lateral offset detected in the radar map, the lane using the lateral offset and lane width detected in the camera image is displayed in blue.

The Particle Filter, see Figure 8, has detected the upcoming curve in frame 94. At this time, the road model represents the actual road course. However, the beginning of the non-clothoidal curve cannot be represented by the clothoid model, the variance of the particles increases. In the curve the stripe

defining the right lane boundary is interrupted due to an outgoing road, which is enclosed by highly reflecting objects. Since the estimated road course is determined by the barycenter of the particles, the straight road course is provided. Between frames 124 and 138 the right curved road courses have a higher probabilities until in frame 139 a right turn cannot be represented by the road model, the estimated road course changes abruptly. At the exit of the road the parameter c_1 does change between frame 199 and 200 but the outgoing road is favored, see frame 222. The correct lane is estimated in frame 245.

The Kalman Particle Filter, see Figure 9, detects the beginning of the curve later than the Particle Filter but the track is not lost and the outgoing road does not influence the estimated road course. In frame 94 the road course shows a tendency to the left side and the estimated curvature changes smoothly. At the exit of the curve between frame 221 and 222 the estimated road course changes fast to keep the track. However, after this no abrupt changes take place.

The curvature estimated by the three filter types are plotted against the driven curvature $c_0 = \frac{\dot{\psi}}{v}$. The results of the Kalman Filter, the Particle Filter and the Kalman Particle Filter are shown in Figure 10. All three filter approaches give a good estimation of the lane course in the straight part, but the curve in frames 150 to 270 highlights the differences of the filter approaches.

The curvature estimated by the Kalman Filter approach is shown in Figure 10a. The plot is very smooth, the apex of the estimated curve is at the same position as the driven curve. But due to missing and wrong measurements at the exit of the curve, there is a significant delay until the correct curvature is estimated. At the straight part of the course the detected curvature is close to the driven one.

The plot showing the curvature estimated by the Particle Filter, see Figure 10b, is close to the driven one at any time. At the beginning, the apex and the exit of the curve, the clothoid parameter c_1 and the curvature alter abruptly. The curvature in the apex is overestimated and the whole plot is not smooth.

In Figure 10c the estimated curvature by the Kalman Particle Filter is shown. The plot is smoother than the result of the Particle Filter and the estimated curvature is closer to the driven one than the result of the Kalman Filter. In contrast to the plot of the Particle Filter approach abrupt variations of c_1 do not occur.

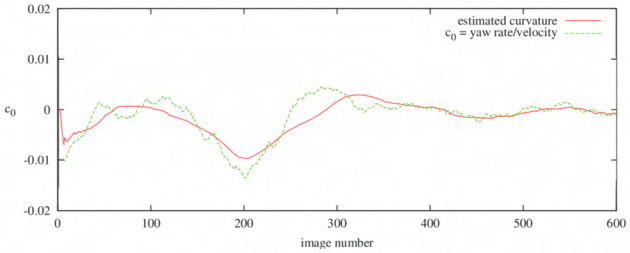

(a) The result of the Kalman Filter is plotted in red. The plot is smooth and the apex of the curve is estimated correctly, but the exit is detected with a significant delay.

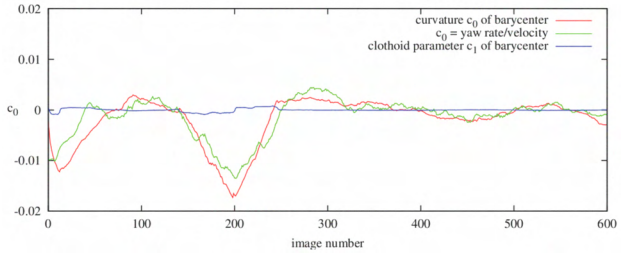

(b) The estimated curvature of the Particle Filter is extracted from the barycenter of the 300 particles and plotted in red. During the whole sequence the estimated curvature is close to the driven one and not smooth at all. The clothoid parameter is shown in blue. It changes abruptly at the beginning, the apex and the exit of the curve, but is zero otherwise.

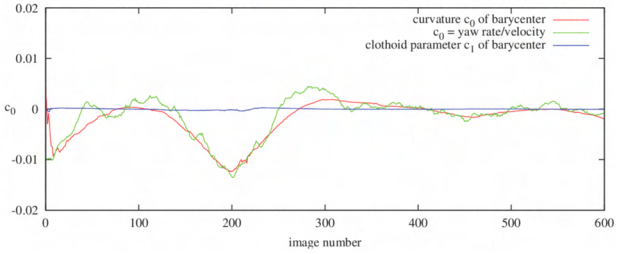

(c) The estimated curvature of the Kalman Particle Filter is plotted in red. In the filter approach 100 particles are used. Only between frame 209 and 221 the curve is not smooth. The other time the curvature changes only slowly.

Fig. 10: Plots of the curvature estimated by the different filter approaches. The green line describes the driven curvature calculated from yaw rate/velocity.

VII. Conclusion and Future Work

By the combination of Kalman and Particle Filter, the Kalman Particle Filter, a mutual support of both filter types is achieved. The Kalman Particle Filter overcomes the limitation of the Kalman Filter, which cannot handle multiple measurements, and the crucial choice of variances in the Particle Filter. The viewing range of an image based lane recognition system is extended with information of radar or stereo evidence grids and due to poorly or unmarked rural roads the Kalman Filter measurements are extracted from these evidence grids. It was shown that the Kalman Particle Filter can be used as a filter for lane recognition algorithms. The estimated curvature changes smoothly like the result of the Kalman Filter, but is close to the driven curvature. Abrupt state variations, which take place using the Particle Filter approach do not occur.

The used clothoid road model does not represent the road course of rural roads very well at large distances. This leads to conflicts between measurements in different viewing ranges and a loss of robustness. Furthermore a planar road is still assumed in our approach but not sufficient for the most rural roads. In [1], [13] and [14] approaches are presented to model the lane in 3D. In our future work a combination of [13] and the presented work is contemplated, but the lane will be modeled in horizontal and vertical direction independently. We will extend the planar clothoid road model by additional road segments and the third dimension for an adequate representation of rural roads.

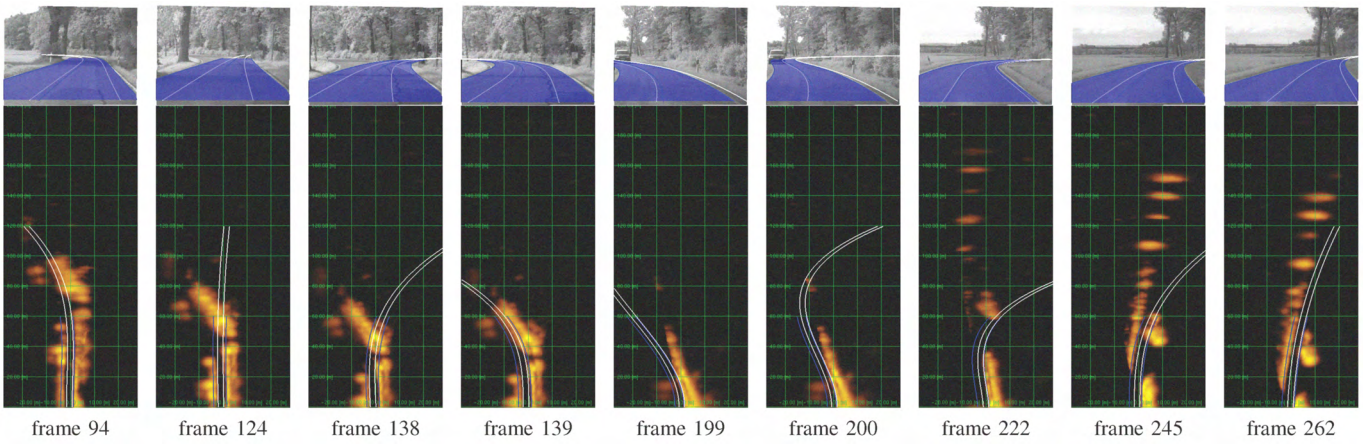

Fig. 8: Estimated road course by Particle Filter: The white lines describe the lane detected in the radar map, the lane detected in the camera image is displayed in blue. The upcoming road is detected already in frame 94, but the track is lost because the clothoid road model does not represent the non-clothoidal curve. The outgoing road at the beginning of the curve leads to a wrong estimation in frame 138. The clothoid parameter c_1 changes abruptly at frame 139. The apex of the curve is detected between frame 199 and 200. But in frame 222 the outgoing road is favored again.

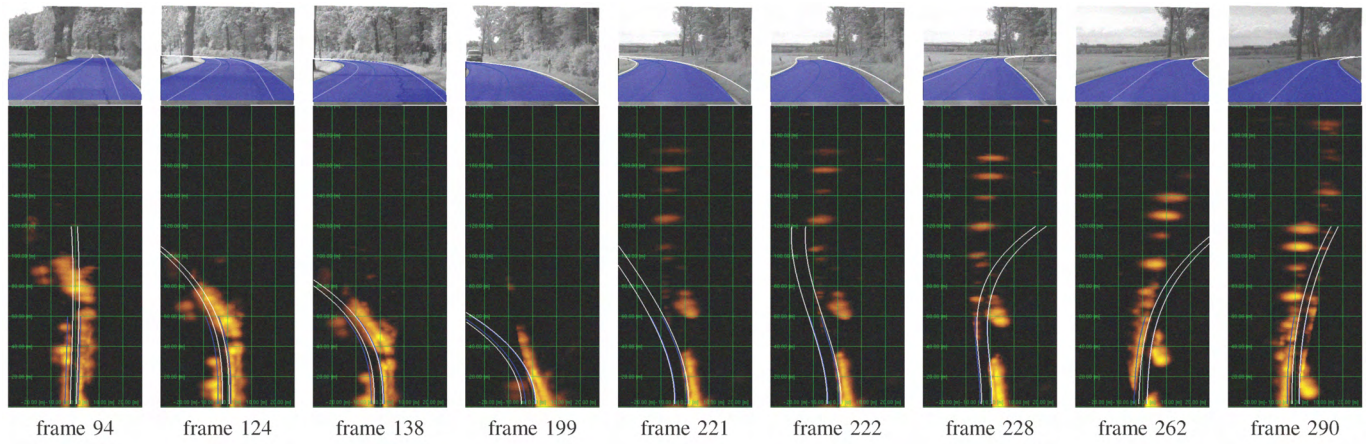

Fig. 9: Estimated road course by Kalman Particle Filter: The white lines describe the lane detected in the radar map, the lane detected in the camera image is displayed in blue. In frame 94 the road course shows a tendency to the left side. The curvature changes smoothly until frame 221, when c_0 and c_1 changes shortly. The outgoing roads do not influence the result of the Kalman Particle Filter.

REFERENCES

[1] E.D. Dickmanns, A. Zapp, *A Curvature-Based Scheme for Improving Road Vehicle Guidance by Computer Vision*, SPIE, vol. 727, pp. 161-168, 1986.

[2] B. Southall, C.J. Taylor. *Stochastic Road Shape Estimation*. In *ICCV01*, 2001, pp. 205-212.

[3] N. Apostoloff, A. Zelinsky. *Robust vision based lane tracking using multiple cues and particle filtering*. In *Proceedings of IEEE Intelligent Vehicles Symposium*, 2003.

[4] P. Smuda, R. Schweiger, H. Neumann, W. Ritter, *Multiple Cue Data Fusion with Particle Filters for Road Course Detection in Vision Systems*. In *Proceedings of IEEE Intelligent Vehicles Symposium*, 2006.

[5] U. Franke, H. Loose, C. Knöppel, *Lane Recognition on Country Roads*. In *Proceedings of IEEE Intelligent Vehicles Symposium*, 2007.

[6] R. Danescu, S. Nedevschi, M.-M. Meinecke, T.-B. To. *A Stereovision-Based Probabilistic Lane Tracker for Difficult Road Scenarios*. In *Proceedings of IEEE Intelligent Vehicles Symposium*, 2008.

[7] U. Meis, R. Schneider, *Radar image acquisition and interpretation for automotive applications*. In *IEEE Intelligent Vehicles Symposium*, 2003, pp. 328-332.

[8] M. Serfling, R. Schweiger, W. Ritter. *Road course estimation in a night vision application using a digital map, a camera sensor and a prototypical imaging radar system*. In *Proceedings of IEEE Intelligent Vehicles Symposium*, 2007.

[9] G. Welch and G. Bishop, *An introduction to the Kalman filter*. Technical report, University of North Carolina at Chapel Hill, Chapel Hill, NC, USA, 1995.

[10] M. Isard, A. Blake, *CONDENSATION – conditional density propagation for visual tracking*. International Journal of Computer Vision, vol. 29, nr. 1, pp. 5-28, 1998.

[11] R. van der Merwe, A. Doucet, N. de Freitas, E. Wan. *The Unscented Particle Filter*. In *num. CUED/F-INFENG/TR 380, Cambridge University Engineering Department*, 2000.

[12] H. Badino, U. Franke, R. Mester. *Free Space Computation Using Stochastic Occupancy Grids and Dynamic Programming*. In *Workshop on Dynamical Vision @ ICCV*, 2007.

[13] A. Wedel, U. Franke, H. Badino, D. Cremers. *B-Spline Modeling of Road Surfaces for Freespace Estimation*. In *Proceedings of IEEE Intelligent Vehicles Symposium*, 2008.

[14] S. Nedevschi, R. Schmidt, T. Graf, R. Danescu, D. Frentiu, T. Marita, F. Oniga, C. Pocol. *3D Lane Detection System Based on Stereovision*. In *Proceedings of IEEE Intelligent Transportation Systems Conference*, 2004.

[15] H. Hirschmüller. *Accurate and Efficient Stereo Processing by Semi-Global Matching and Mutual Information*. CVPR 2005, PAMI 30(2):328-341, 2008.

[16] S. K. Gehrig, U. Franke. *Improving Stereo Sub-Pixel Accuracy for Long Range Stereo*. ICCV VRML workshop 2007.